https://doi.org/10.17221/191/2020-VETMED

Intracranial meningioma in a pet rat: MRI findings

Ciro Cococcetta[1], Francesca Del Signore[1], Ilaria Cerasoli[1], Giovanni Di Guardo[1], Marina Baffoni[1], Gabriella Di Francesco[2], Veronica Crocchianti[1], Massimo Vignoli[1]*

[1]*Veterinary Teaching Hospital, University of Teramo, Teramo, Italy*
[2]*Istituto Zooprofilattico Sperimentale dell'Abruzzo e Molise "G. Caporale", Teramo, Italy*

**Corresponding author: cirococ@gmail.com*

Citation: Cococcetta C, Del Signore F, Cerasoli I, Di Guardo G, Baffoni M, Di Francesco G, Crocchianti V, Vignoli M (2021): Intracranial meningioma in a pet rat: MRI findings. Vet Med-Czech 66.

Abstract: We herein report the magnetic resonance imaging (MRI) findings in a brain meningioma in a pet rat (*Rattus norvegicus domestica*). A 1.5-year-old pet rat was referred for depression, ataxia, tremors and bilateral nystagmus; a brain MRI was elected suspecting an intracranial neoplasia. The study was performed with a 0.25 T scanner. The MRI revealed a well-defined oval mass with a heterogeneous appearance, hyperintense in T1 and T2, and with extra-axial localisation and severe brain compression, the mass appeared strongly and diffusely contrast-enhancing. Euthanasia was elected, with the necropsy confirming the presence of a voluminous extra-axial mass. Histologically, a well-differentiated, benign meningotheliomatous meningioma was diagnosed, with the histochemical stains allowing one to exclude a granular cell tumour. To the best of our knowledge, this is the first report of MRI investigations on a pet rat intracranial meningioma.

Keywords: benign meningotheliomatous meningioma; brain tumour; magnetic resonance imaging; *Rattus norvegicus*

Meningiomas represent the most commonly reported primary brain tumour in dogs and cats (Troxel et al. 2003; Snyder et al. 2006), arising from the cap cells covering the arachnoid granulations, particularly at the point where they project into the venous sinuses (Summer et al. 1995).

Although meningioma is known in rats, most of the information available on spontaneous cases of such neoplasia comes from post-mortem investigations on laboratory rats, being related only to a specific rat strain (Mitsumori et al. 1988). Furthermore, while meningioma-related magnetic resonance imaging (MRI) findings are thoroughly described in dogs and cats (Wisner et al. 2011), no information about MRI findings in naturally occurring meningiomas is available in rats.

The aim of the present study is to describe MRI and microscopic findings in a brain meningioma in a pet rat (*Rattus norvegicus domestica*).

Clinical case

A 1.5-year-old pet rat was referred for weight loss, depression and episodes of rolling. The rat had already undergone radiographic and haematobiochemical examinations, which yielded inconsistent results.

The physical examination highlighted a body condition score of 2 out of 5, and dehydration of more than 10%, assessed by skin turgor. The neurological examination revealed ataxia, tremors and bilateral vertical nystagmus; no alterations were observed during the peripheral nerve examination. Based on these findings, an intracranial mass was suspected and, consequently, a brain MRI study was performed.

The patient was anaesthetised with Isoflurane (IsoFlo fl 250 ml isoflurane; Zoetis Italy srl, Milano, Italy) at 4% (vaporising setting) with a fresh gas flow

https://doi.org/10.17221/191/2020-VETMED

of 2 l/min inside a handcraft induction chamber; once anaesthetised, the rat was intubated using a 2.5 uncuffed endotracheal tube and maintained at an end tidal isoflurane of 1% for the procedure. The right tarsal vein of the patient was catheterised (Deltaven® 26G × 19 mm; Delta Med Italy srl, Viadana, Italy) and fluid therapy was intravenously administered at the infusion rate of 10 ml/kg/h. The MRI study was performed using a 0.25 T Esaote Vetscan Grande scanner using a foot/ankle coil 4 (Esaote SpA, Genova, Italy). The scanning protocol comprised SE T1w on the sagittal (TR 560, TE 26, gap 0, FOV 240 × 240, matrix 480 × 400) and transverse (TR 560, TE 26, gap 0, FOV 180 × 180, matrix 352 × 304) planes, FSE T2w on the sagittal (TR 2 600, TE 90, gap 0, FOV 220 × 220, matrix 480 × 352) and transverse (TR 3 170, TE 90, gap 0, FOV 210 × 200, matrix 448 × 305) planes, and FLAIR sequences on the dorsal plane (TR 3 410, TE 90, gap 0, FOV 150 × 120, matrix 288 × 179), followed by a post-contrast transverse SE T1w (0.3 ml/kg Magnegita-Gadopentetate dimeglumine 500 µmol/ml; Agfa HealthCare Imaging Agents GmbH, Köln, Germany); all the sequences were performed at a 3 mm slice thickness.

A well-defined oval mass of 0.7 cm dorsoventral × 1.1 cm rostrocaudal × 0.8 cm mediolateral with extra-axial localisation was detected with the MRI examination; the entire brain parenchyma appeared to be severely compressed, with *falx cerebri* being displaced to the right side of the brain.

The lesion appeared heterogeneous and slightly hyperintense on the T1w and FLAIR images and strongly hyperintense on the T2w images (Figure 1). No herniation or dural tail were recorded, but in the T2w and in FLAIR, hypointense areas rostral and to the right to the mass was detected, thus justifying a suspected perilesional haemorrhage.

Furthermore, iso-hyperintense, heterogeneous and amorphous material was observed in the left tympanic bulla; thereby confirming a diagnosis of concurrent unilateral otitis media.

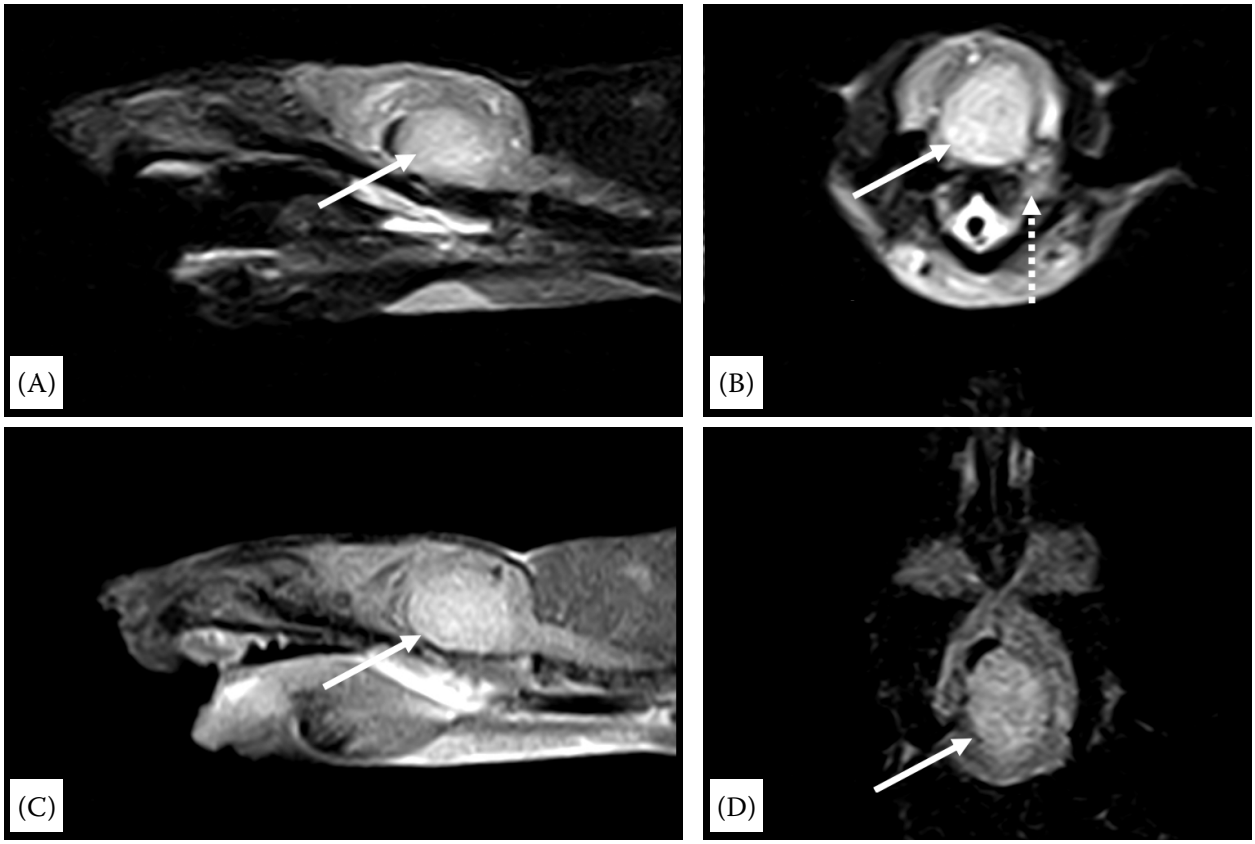

Figure 1. FSE T2w sagittal (A) and transverse (B) images of the brain mass characterised by a hyperintense and heterogeneous aspect (solid white arrow). SE T1w Sagittal (C) and FLAIR dorsal images (D) of the brain mass; notice the hyperintense aspect in both the sequences (solid white arrow)

In the FSE T2 W and FLAIR images, a hypointense area is evident rostral to the mass and in the FSE T2w transverse, iso-hyperintense and amorphous material is observed in the right tympanic bulla (dotted white arrow)

https://doi.org/10.17221/191/2020-VETMED

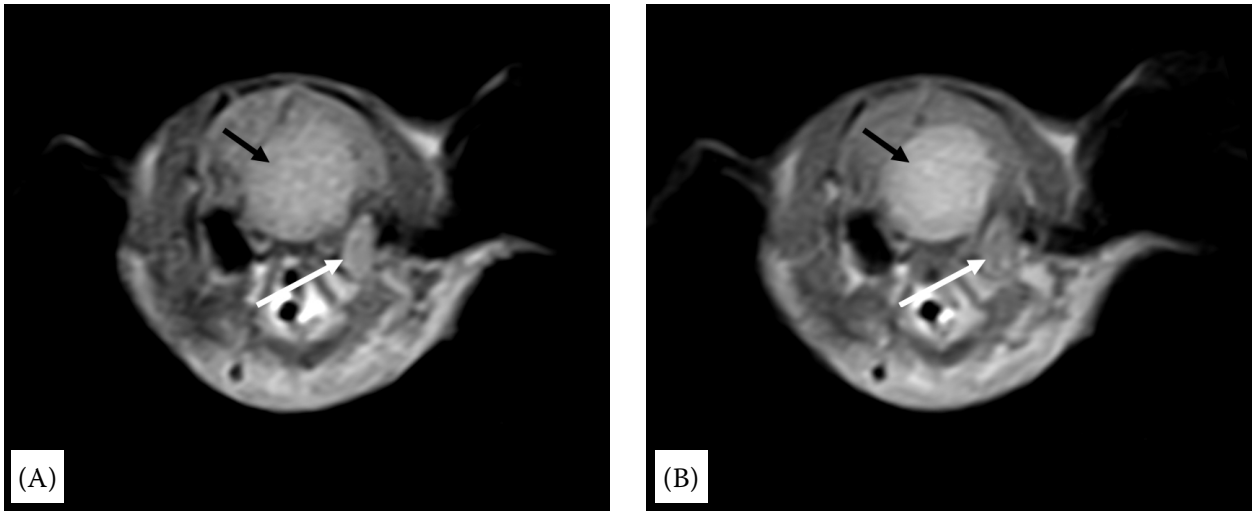

Figure 2. SE T1w transverse images before (A) and after (B) contrast; the mass is strongly and diffusely enhanced (black arrow)

In the left tympanic bulla, amorphous and heterogeneous material is observed, without contrast enhancement (white arrow)

Following contrast administration, a strong and diffuse enhancement was detected around the oval mass (Figure 2). Neoplasia was suspected with the most likely diagnosis being consistent with a meningioma. Indeed, an abscess and a granuloma were excluded due to the diffuse contrast enhancement. The owner was duly informed and elected euthanasia. Following euthanasia (Tanax®; Msd Animal Health Srl, Segrate, Italy), a detailed post-mortem examination was performed, with all the major organs from the rat being promptly fixed in 10% neutral buffered formalin for the histopathological investigations. Once properly fixed, the entire brain was cut into horizontal slices, which were embedded in paraffin and cut into 5 micron-thick sections. These were subsequently stained with haematoxylin and eosin (H&E), with a number of brain sections being additionally stained with periodic acid Schiff (PAS) and Perls' haemosiderin histochemical techniques. Macroscopically, a well-circumscribed, large and brownish red mass was observed, with this lesion exhibiting a uniform and moderately firm consistency, while exerting a marked compression on the neighbouring and underlying cerebral parenchyma, more than half of which appeared to be in close contact with the tumour mass (Figure 3).

Histologically, the lesion was composed by a dense population of substantially homogeneous neoplastic cells, conferring to the mass a "papillary-like" morphological appearance, intermingled with a "pseudo-lobular" pattern. These papillary-like and pseudo-lobular areas were frequently centred by more or less enlarged spaces consistent with vascular *lumina*, around which the neoplastic proliferation was apparently growing. The tumour elements showed distinct borders and large clear nuclei harbouring single prominent nucleoli, along with scanty agranular cytoplasms showing no evidence of PAS-positive granules. Few mitotic figures (less than 1/HPF, on average) were additionally observed, with no evidence of nuclear atypia and nucleocytoplasmic polymorphism. Isolated necrotic le-

Figure 3. Rat (*R. norvegicus*) brain

Post-mortem macroscopic view of the voluminous mass compressing the adjacent and underlying neuroparenchyma, more than half of which appears to be in close contact with the tumour mass

https://doi.org/10.17221/191/2020-VETMED

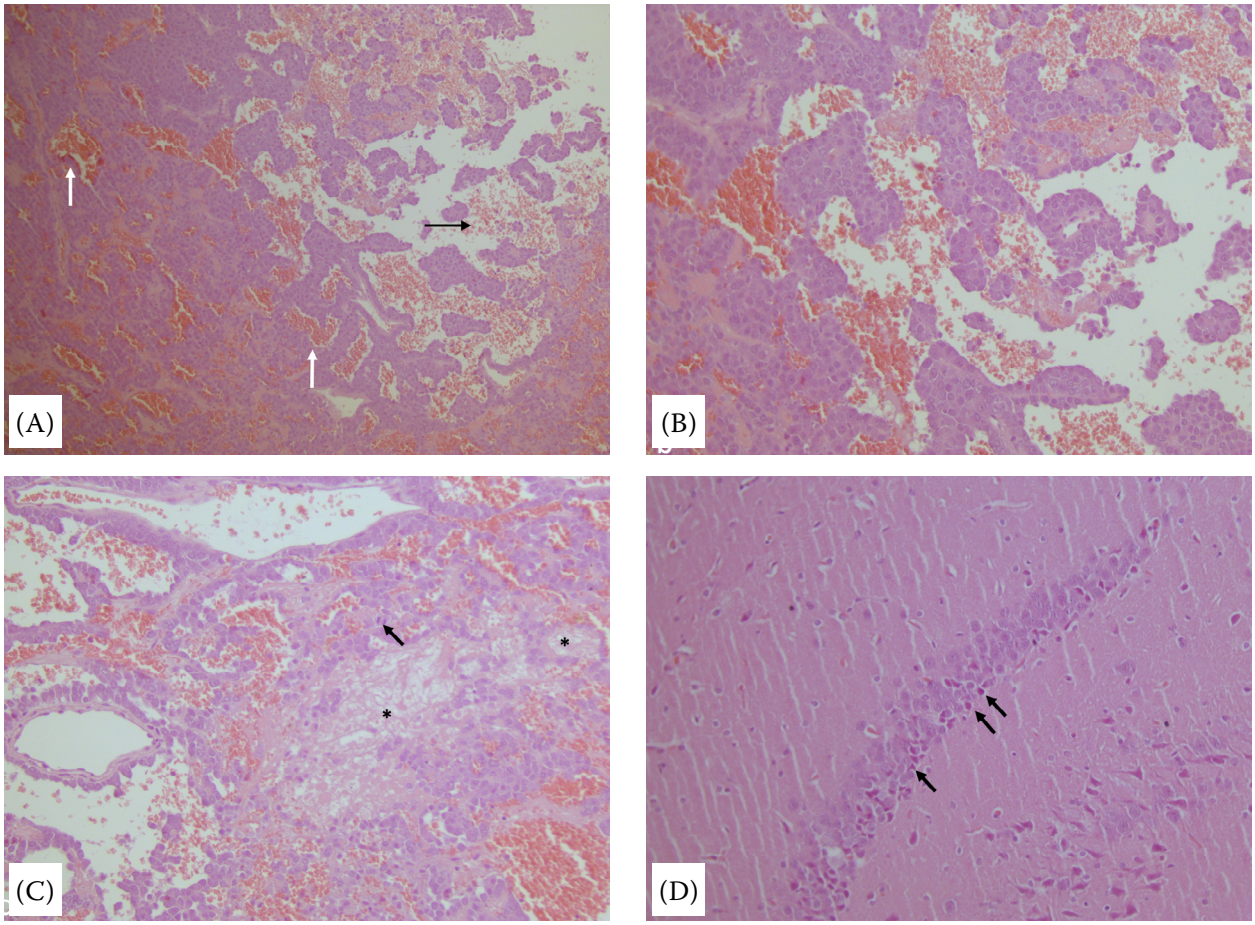

Figure 4. Rat (*R. norvegicus*) brain meningioma
(A) The neoplastic tissue architecture shows a "papillary" pattern, intermingled with a "pseudo-lobular/lobulated/solid" lesion pattern. Blood-filled vascular lumina (white arrows) and haemorrhagic foci (black arrow) are also apparent within the neoplasia. Haematoxylin and eosin (H&E) stain, × 100. (B) At higher magnification, the neoplasia appears to be composed of papillae, cords and/or nests of well-differentiated, round-to-oval cells with large clear nuclei harbouring single prominent nucleoli and a scanty cytoplasm. H&E stain, × 200. (C) Evidence of necrotic foci (asterisks) alongside occasional mitotic cell figures (black arrow) is shown within the neoplastic parenchyma. H&E stain, × 200. (D) Several neurons from the hippocampal region appear to be damaged (black arrows), thereby exhibiting a "shrunken" morphology ("dark" neurons). H&E stain, × 200

sions, coupled with recent haemorrhagic foci, could also be found within the neoplasia, which did not infiltrate the adjacent brain parenchyma. The latter showed, in turn, neurodegenerative changes, especially at the level of hippocampal (*gyrus dentatus*) neurons, which frequently showed peripheral chromatolysis and, sometimes, a "dark (shrunken) neuron" morphology. A very scant haemosiderin pigment deposition was also observed at the level of the aforementioned haemorrhagic lesions (Figure 4).

Based on the reported MRI herein and the histopathological findings, a final diagnosis of a well-differentiated, benign meningotheliomatous meningioma was made.

DISCUSSION

We have herein described the MRI findings of a brain meningioma in a rat, a species being increasingly considered as a pet. Very few articles are available on the clinical and diagnostic features of meningiomas in pet rats. Moreover, no previous works have been published about the clinical and diagnostic features of this pathology in a pet rat and also low-field MRI scanner applications to brain disorders in this species are rarely reported (Breton et al. 2008).

Spontaneous brain neoplasms in this species represent less than 1% of the tumours (Sumi et al.

https://doi.org/10.17221/191/2020-VETMED

1976), with a high prevalence of meningiomas diagnosed post-mortem without imaging investigations (Dagle et al. 1979). In this latter study, 1.4% of all rat tumours were in the brain, with most of them being astrocytomas followed by ependymomas, meningiomas, pinealomas, reticuloses, oligodendrogliomas and gliomatoses. Similar findings were reported in other studies, with astrocytomas being diagnosed in 0.53% of females and 1.04% of males (Chandra et al. 1992) as well as in 0.9% of Sprague-Dawley rats affected by neoplasia (Prejean et al. 1973). In another study, a total of 8 960 Sprague-Dawley-derived rats (strain TZRAI) were analysed, with the histopathology revealing 90 primary brain neoplasms, namely 55 granular cell meningiomas, 19 reticuloses, 11 neuroglial tumours, 4 pineal tumours and 1 pleomorphic meningeal sarcoma (Krinke et al. 1985).

Regarding the canine and feline species, meningiomas are quite common endocranial tumours (Motta et al. 2012; Bentley 2015). MRI findings include round-to-ovoid or plaque-like, usually well-defined masses associated with the brain, typically in broad-based contact with the underlying bone (Sumi et al. 1976; Hathcock 1996; Kraft et al. 1997; Troxel et al. 2004; Wisner and Zwingerberger 2015).

The neoplasia typically appears hypointense to isointense on T1w images, hyperintense on T2w and FLAIR images, thereby showing diffuse and strong contrast enhancement in 60–70% of cases with thickening of the meninges adjacent to the tumour (dural tail sign) (Graham et al. 1998; Wisner et al. 2011).

The herein described neoplasm shares most of the MRI imaging findings reported for canine and feline brain meningiomas, with special emphasis on the ovoid shape and the diffuse and robust contrast enhancement, without considering the extra-axial location (Hathcock 1996).

On the contrary, a diffuse and slight hyperintense signal has been detected with the T1w sequences and the reason for this particular feature may be justified by the presence of haemorrhagic lesions detected by the histopathology, since subacute haemorrhages appear typically hyperintense in both T1w and T2w sequences (McConnell 2018).

Moreover, while hyperostosis is a well described feature in cats affected by this kind of neoplasia (Troxel et al. 2003), this finding was not observed in our case.

In dogs, intracranial meningiomas may invade the middle ear (Owen et al. 2004), but in this case, otitis media was simultaneously diagnosed, since no contrast enhancement was detected, and no abnormalities were macroscopically observed in the tympanic bulla.

Furthermore, as far as the histomorphological features of the well-differentiated benign meningotheliomatous meningioma in the herein investigated pet rat is concerned, they appear to be entirely consistent with those previously described in the human and domestic animal disease "counterparts", according to the "WHO Classification of Tumours" (Sturges et al. 2008). In this respect, the lesion's histomorphological features allowed us to clearly differentiate it from a meningeal "granular cell tumour" (GCT), despite the frequently reported occurrence of the latter in rats (Mitsumori et al. 1987). Rat meningeal GCTs are composed, in fact, by a predominant population of large pleomorphic cells with large vesicular nuclei harbouring small nucleoli and with abundant cytoplasms containing PAS-positive granules, intermingled with less numerous small cells containing small dense nuclei and scant agranular cytoplasms in rats (Mitsumori et al. 1987).

With reference to the necrotic and haemorrhagic foci observed within the neoplastic parenchyma, they could have resulted from the compression exerted by the tumour on the surrounding tissue components or, alternatively, from blood vessel erosion due to progressive neoplastic tissue expansion. In more detail, the aforementioned haemorrhages should be interpreted as predominantly recent lesions, given the scanty haemosiderin deposition found inside and around them. The same could also apply to neuronal damage in the neighbouring hippocampal region, since no microglial cell aggregates were apparent at that level.

The main limitation of the present study is the relatively low definition of the MRI images, since a low-field scanner was used in this case. While these instruments are widely in use in veterinary facilities because of their high versatility and their relatively limited costs, the signal-to-noise ratio (SNR) is low, and this aspect negatively influences the quality and the spatial resolution of the images, especially in small sized patients (Konar and Lang 2011).

Since these instruments are potentially applicable to a large scale also in exotic pet medicine, this fea-

https://doi.org/10.17221/191/2020-VETMED

ture needs to be fully considered and proper technical settings need to be set in order to maximise the quality of images, taking the normal anatomy that can be visualised with this kind of scanner into account.

While rat brain anatomy has been investigated with high field MRI scanners (Schwarz et al. 2006), a detailed description of what can be visualised in this species with low field scanners is currently missing, with reports being available only for the mouse brain (Choquet et al. 2009).

In conclusion, to our knowledge, this is the first report of an MRI used to diagnose a spontaneous intracranial meningioma in a pet rat.

Further studies are needed to fully characterise the clinical prevalence of this kind of neoplasia in a species increasingly considered as a pet, thus making advanced imaging studies extremely useful to investigate endocranial disorders even in small sized patients.

Conflict of interest

The authors declare no conflict of interest.

REFERENCES

Bentley RT. Magnetic resonance imaging diagnosis of brain tumors in dogs. Vet J. 2015 Aug;205(2):204-16.

Breton E, Goetz C, Choquet P, Constantinesco A. Low field magnetic resonance imaging in a rat in vivo. IRBM. 2008 Dec;29(6):366-74.

Chandra M, Riley MG, Johnson DE. Spontaneous neoplasms in aged Sprague-Dawley rats. Arch Toxicol. 1992; 66(7):496-502.

Choquet P, Breton E, Goetz C, Marin C, Constantinesco A. Dedicated low-field MRI in mice. Phys Med Biol. 2009 Sep;54(17):5287-99.

Dagle GE, Zwicker GM, Renneal RA. Morphology of spontaneous brain tumors in the rat. Vet Pathol. 1979;16(3): 318-24.

Graham JP, Newell SM, Voges AK, Roberts GD, Harrison JM. The dural tail sign in the diagnosis of meningiomas. Vet Radiol Ultrasound. 1998 Jul-Aug;39(4):297-302.

Hathcock JT. Low field magnetic resonance imaging characteristics of cranial vault meningiomas in 13 dogs. Vet Radiol Ultrasound. 1996 July;37(4):257-63.

Konar M, Lang J. Pros and cons of low-field magnetic resonance imaging in veterinary practice. Vet Radiol Ultrasound. 2011 Mar-Apr;52(Suppl 1):S5-S14.

Kraft SL, Gavin PR, DeHaan C, Moore M, Wendling LR, Leathers CW. Retrospective review of 50 canine intracranial tumors evaluated by magnetic resonance imaging. J Vet Intern Med. 1997 Jul-Aug;11(4):218-25.

Krinke G, Naylor DC, Schmid S, Frohlich E, Schnider K. The incidence of naturally-occurring primary brain tumours in the laboratory rat. J Comp Pathol. 1985 Apr; 95(2):175-92.

McConnell FJ. Brain hemorrhage. In: Wilfried M, editor. Diagnostic MRI in dogs and cats. 1st ed. Boca Raton, FL: CRC Press; 2018. p. 286.

Mitsumori K, Maronpot RR, Boorman GA. Spontaneous tumors of the meninges in rats. Vet Pathol. 1987 Jan; 24(1):50-8.

Mitsumori K, Stefanski SA, Maronpot RR. Benign and malignant neoplasms, meninges, rat. In: Jones TC, Mohr U, Hunt RD, editors. Nervous system. Berlin: Springer; 1988. p. 108-17.

Motta L, Mandara MT, Skerritt GC. Canine and feline intracranial meningiomas: An updated review. Vet J. 2012 May;192(2):153-65.

Owen MC, Lamb CR, Lu D, Targett MP. Material in the middle ear of dogs having magnetic resonance imaging for investigation of neurologic signs. Vet Radiol Ultrasound. 2004 Mar-Apr;45(2):149-55.

Prejean JD, Peckham JC, Casey AE, Griswold DP, Weisburger EK, Weisburger JH. Spontaneous tumors in Sprague-Dawley rats and Swiss mice. Cancer Res. 1973 Nov;33(11): 2768-73.

Schwarz AJ, Danckaert A, Reese T, Gozzi A, Paxinos G, Watson C, Merlo-Pich EV, Bifone A. A stereotaxic MRI template set for the rat brain with tissue class distribution maps and co-registered anatomical atlas: Application to pharmacological MRI. Neuroimage. 2006 Aug 15;32(2):538-50.

Snyder JM, Shofer FS, Van Winkle TJ, Massicotte C. Canine intracranial primary neoplasia: 173 cases (1986–2003). J Vet Intern Med. 2006 May-Jun;20(3):669-75.

Sturges BK, Dickinson PJ, Bollen AW, Koblik PD, Kass PH, Kortz GD, Vernau KM, Knipe MF, Lecouteur RA, Higgins RJ. Magnetic resonance imaging and histological classification of intracranial meningiomas in 112 dogs. J Vet Intern Med. 2008 May-Jun;22(3):586-95.

Sumi N, Stavrou D, Frohberg H, Jochmannal G. The incidence of spontaneous tumors of the central nervous system of wistar rats. Arch Toxicol. 1976;35(1):1-13.

Summer BA, Cummings JF, DeLahunta A. Tumours of the central nervous system. In: Summer BA, Cummings JF, DeLahunta A, editors. Veterinary neuropathology. St. Louis: Mosby; 1995. p. 351-401.

Troxel MT, Vite CH, Van Winkle TJ, Newton AL, Tiches D, Dayrell-Hart B, Kapatkin AS, Shofer FS, Steinberg SA.

https://doi.org/10.17221/191/2020-VETMED

Feline intracranial neoplasia: Retrospective review of 160 cases (1985–2001). J Vet Intern Med. 2003 Nov-Dec;17(6):850-9.

Troxel MT, Vite CH, Massicotte C, McLear RC, Van Winkle TJ, Glass EN, Tiches D, Dayrell-Hart B. Magnetic resonance imaging features of feline intracranial neoplasia: Retrospective analysis of 46 cats. J Vet Intern Med. 2004 Mar-Apr;18(2):176-89.

Wisner ER, Dickinson PJ, Higgins RJ. Magnetic resonance imaging features of canine intracranial neoplasia. Vet Radiol Ultrasound. 2011 Mar-Apr;52(Suppl 1):S52-61.

Wisner ER, Zwingerberger AL. Brain. In: Wisner ER, Zwingerberger AL, editors. Atlas of small animal CT and MRI. Ames: Wiley Blackwell; 2005. p. 153-278.

Received: September 25, 2020
Accepted: April 20, 2021